

Research Report

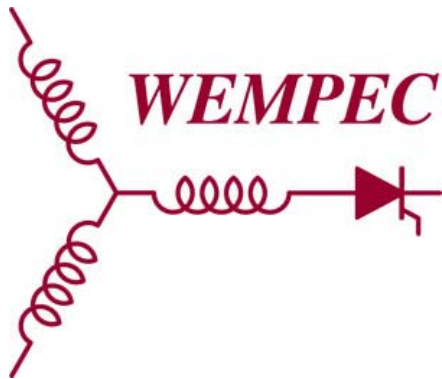
2014-30

**Optimal Design of a Novel V-type IPM Motor with Assisted Barriers  
for the Improvement of Torque Characteristics**

**W. Zhao, T.A. Lipo\*, B. Kwon**

Department of Electronic Systems  
Engineering,  
Hanyang University,  
Ansan-si, Gyeonggi-do, 426-791, Korea

\* Department of Electrical and Computer  
Engineering,  
University of Wisconsin-Madison,  
Madison, WI, 53706-1691, USA



**Wisconsin  
Electric  
Machines &  
Power  
Electronics  
Consortium**

University of Wisconsin-Madison  
College of Engineering  
Wisconsin Power Electronics Research Center  
2559D Engineering Hall  
1415 Engineering Drive  
Madison WI 53706-1691

© Confidential

# Optimal Design of a Novel V-type IPM Motor with Assisted Barriers for the Improvement of Torque Characteristics

Wenliang Zhao<sup>1</sup>, Thomas A. Lipo<sup>2</sup>, *Life Fellow, IEEE*, and Byung-il Kwon<sup>1</sup>, *Senior Member, IEEE*

<sup>1</sup>Department of Electronic Systems Engineering, Hanyang University, Ansan, 426-791, Korea

<sup>2</sup>Department of Electrical and Computer Engineering, University of Wisconsin-Madison, Madison, WI 53706-1691, USA

This paper performs a study on the optimal design of V-type interior permanent magnet motors (VIPMMs) in which the rotor is equipped with assisted barriers for the improvement of average torque and torque ripple. The approach differs from conventional IPM motors in which the reluctance torque due to saliency reaches a maximum value at a current phase angle located 45 electrical degrees with respect to the maximum value obtained from the magnetic PM torque produced by the rotor magnets. Adoption of assisted barriers is employed to improve the torque production by making rotor asymmetric making the reluctance torque and the magnetic torque reach a maximum near or at the same current phase angle. In order to evaluate the contribution, the frozen permeability method (FPM) is utilized to segregate the torque into its reluctance and magnetic torque components. Firstly, an iterative optimization is performed on a concept design of a 6/4 VIPMM for demonstrating the design principle. Then the VIPMM is further optimized by algorithms such as Kriging method and genetic algorithm (GA) for improving the torque characteristics and efficiency. The optimal motor with assisted barriers shows substantially improved performance compared to a conventional design.

**Index Terms**—Finite element method (FEM), frozen permeability method (FPM), genetic algorithm (GA), magnetic torque, optimal design, torque, torque ripple, V-type interior permanent magnet motors (VIPMMs).

## I. INTRODUCTION

IN recent years, interior permanent magnet motors (IPMMs) have been comprehensively investigated for many applications due to their high efficiency, high torque density and wide operating range [1]-[3]. In these works it has been shown that the V-type IPMM contains a higher saliency ratio and lower PM losses than the flat type, making it more suitable for high speed applications especially for electric vehicles [4]. However, further improved performance is generally always desirable.

An extensive literature with various techniques can be found for improving the performance of IPMMs [5]-[7]. In particular, the flux barrier design has been recognized as an effective solution when applied to the reduction of torque ripple rather than the improvement of average torque [8]. It is well known that one of the significant features in IPMMs is the presence of magnetic saliency which contributes to the production of reluctance torque, resulting in enhanced torque and efficiency combining with the magnetic torque from the rotor magnets. By convention, an elegant d-q rotor frame equivalent circuit can be developed for analyzing the torque components using Park transformation, where it is displayed that the magnetic torque and the reluctance torque reach the maximum value at different current phase angles theoretically by 45 electrical degrees with respect to each other. Consequently, the resultant torque is obtained as the vector sum of the two components rather than the algebraic sum. Hence, only a portion of each torque component is effectively utilized in any known IPMM design previously reported.

In this paper, a novel V-type IPM motor with assisted barriers between two adjacent poles is proposed for improving

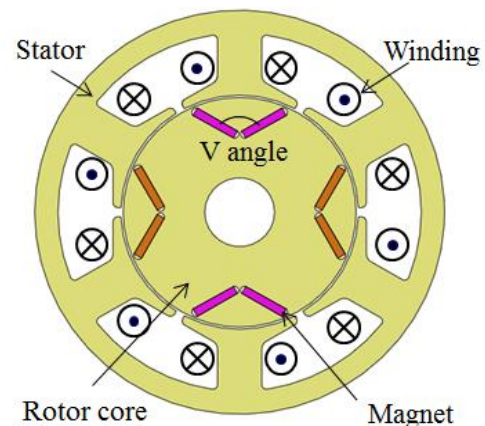


Fig. 1. Configuration of the conventional V-type IPM motor.

torque characteristics by making the magnetic torque and the reluctance torque reach its maximum near or at the same current phase angle. In order to provide valuable insights to the contribution, the frozen permeability method (FPM) is utilized to separate the torque into the reluctance torque and magnetic torque based on a 2-D time stepping finite element method (FEM) [9], [10]. Firstly, an iterative optimization is performed on the concept design of a 6/4 VIPMM for demonstrating the design principle. Then the VIPMM is optimized by algorithms such as the Kriging method and a genetic algorithm (GA) for further improving the torque characteristics and efficiency. The consequent optimal results show that the performance of the optimal motor with assisted barriers has been substantially improved.

## II. CONCEPT DESIGN

### A. Typical Torque Characteristics of VIPMM

Fig. 1 shows the configuration of the conventional V-type IPM motor. The stator has 6 slots with concentrated winding. The ferrite magnets buried in the rotor are arranged as V shape.

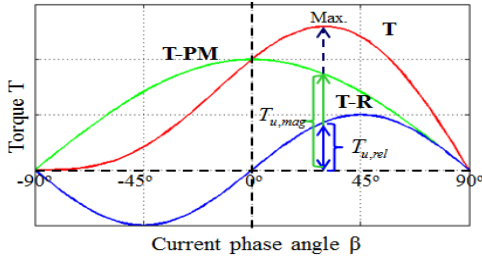


Fig. 2. Typical torque characteristics. T: Resultant torque, T-PM: Magnetic torque, T-R: Reluctance torque.

The electromagnetic torque obtained from the d-q rotating reference frame can be expressed as

$$T = \frac{3p}{2} [\lambda_{pm} I_a \cos \beta + \frac{1}{2} (L_d - L_q) I_a^2 \sin 2\beta] \quad (1)$$

where  $p$  is the number of pole pairs,  $\beta$  is the spatial angle of the stator current vector measured with respect to the q-axis,  $L_d$  and  $L_q$  are the inductances of the d- and q-axes respectively,  $I_a$  is the peak value of phase current and  $\lambda_{pm}$  is the peak fundamental value of magnet flux linking the stator windings. The first term in (1) is termed the magnetic torque while the second term is the reluctance torque due to the saliency.

Frozen permeability method (FPM) is utilized to separate the torque into the reluctance torque and magnetic torque based on finite element method (FEM). The reluctance torque was firstly obtained by removing the magnets. Then the magnets were inserted and the resultant torque determined. The magnetic torque was then calculated by subtracting the reluctance torque from the resultant torque. The typical torque characteristics based on (1) are shown in Fig. 2. A utilization factor (UF) is defined as the ratio of the utilized magnetic or reluctance torque component contributing to the maximum torque and its corresponding peak torque component, and can be expressed as

$$UF_{mag} = \frac{T_{u,mag}}{T_{pk,mag}}; UF_{rel} = \frac{T_{u,rel}}{T_{pk,rel}}; \quad (2)$$

where  $T_{u,mag}$  and  $T_{u,rel}$  are the utilized magnetic torque and the utilized reluctance torque which contribute to the maximum resultant torque as shown in Fig. 2 respectively.  $T_{pk,mag}$  and  $T_{pk,rel}$  are the peak values of each torque components.

### B. Concept Design

As opposed to conventional design techniques, the improvement of the torque production in this paper is achieved by making the reluctance torque and the magnetic torque reach their maximum near or at the same current phase angle. In order to demonstrate the design principle, an iterative optimization can be firstly performed on the concept design.

Fig. 3 shows the motors that were investigated. The basic motor with the V-angle of 50 degrees is shown in Fig. 3(a), and the proposed motor with the design variable selected as the open angle of the assisted barrier  $\gamma$  is shown in Fig. 3(b). The motor specification is listed in Table I. The rated speed is 4800 rpm. The torque characteristics are analyzed by feeding with 3 phase sinusoidal current excitation at the current density of 3 Arms/mm<sup>2</sup>. The optimization criterion is to make the UF of each torque component as unity. By an iterative optimization process, a value of UF as unity occurs at  $\gamma=27^\circ$ .

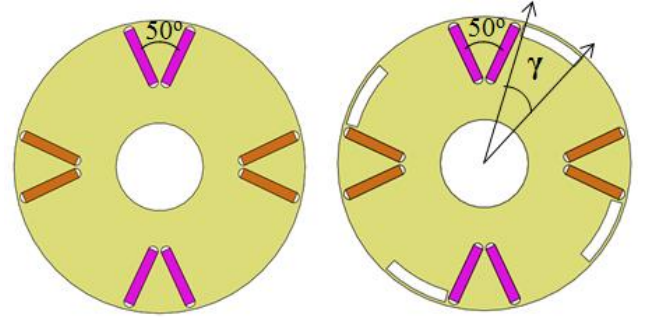


Fig. 3. VIPM motors in concept design.

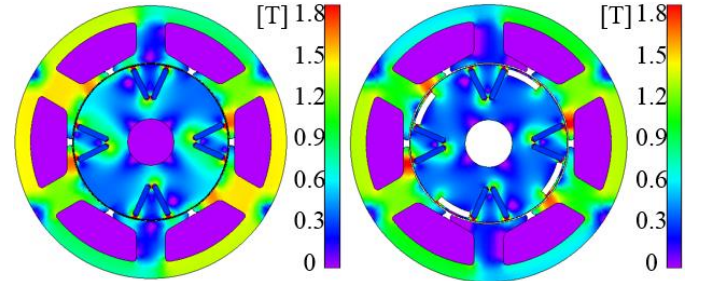


Fig. 4. Magnetic flux density distribution.

TABLE I  
SPECIFICATION OF THE INVESTIGATED MOTOR

Item	Unit	Value
Number of magnet poles	-	4
Number of stator slots	-	6
Stator outer diameter	mm	88
Stator inner diameter	mm	51
Airgap length	mm	0.5
Rotor outer diameter	mm	50
Rotor inner diameter	mm	15
Lamination axial length	mm	52
Remanence of Ferrite PM	T	0.41

The magnetic flux density distribution for both motors is shown in Fig. 4 which shows that the proposed motor with assisted barriers improves the magnetic flux density distribution as compared with the basic motor. Fig. 5 shows the torque characteristics of both motors. The two torque components reach its maximum torque at different current phase angles in basic motor as shown in Fig. 5(a), while it shows that the two torque components of the proposed motor reach the maximum value at the same current phase angle which improves the resultant torque dramatically as shown in Fig. 5(b). The maximum resultant torque for proposed motor has increased by over 35.5% from that of basic motor demonstrating a superior result using the same amount of magnet material. The efficiency has also increased by 6.3% due to the improvement of torque and the reduction of iron loss. The efficiency is herein defined as

$$\eta = \frac{P_{out}}{P_{out} + P_{copper} + P_{iron}} \quad (3)$$

where  $P_{out}$  is the output power,  $P_{copper}$  is the copper loss and  $P_{iron}$  is the iron loss in the stator and rotor core.

Fig. 6 shows the comparison of electromagnetic torque. The torque ripple factor is defined as the ratio of peak to

TABLE II  
COMPARISON OF PERFORMANCE DATA IN CONCEPT DESIGN

Item	Unit	Basic motor	Proposed motor
Max. torque (AVG)	Nm	0.307	0.416
UF of reluctance torque	%	83.1	100
UF of magnetic torque	%	99.2	100
Torque ripple	%	166.1	131.2
Output power	W	154.3	209.1
Copper loss	W	9.6	
Iron loss	W	19.56	15.28
Efficiency	%	84.1	89.4

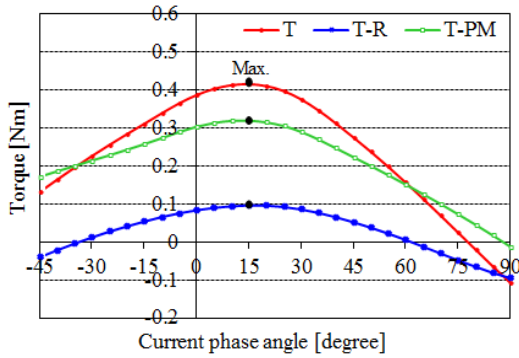
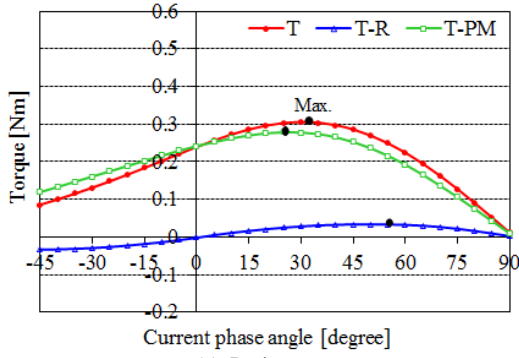


Fig. 5. Torque characteristics. T: Resultant torque, T-PM: Magnetic torque, T-R: Reluctance torque.

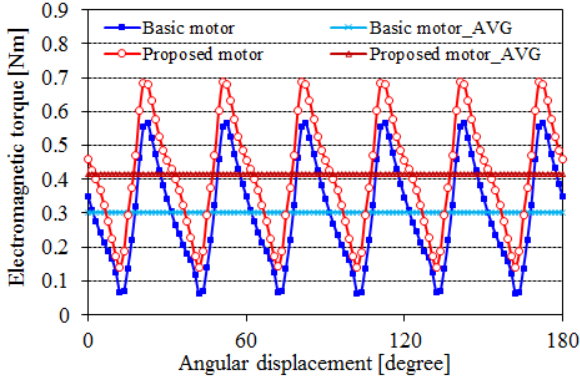


Fig. 6. Electromagnetic torque of the basic and proposed motors.

peak torque value to average torque value as

$$K_T = \frac{T_{max} - T_{min}}{T_{AVG}} \quad (4)$$

The torque ripple factor of the proposed motor is decreased by 21.7%, and the detailed data is summarized in Table II.

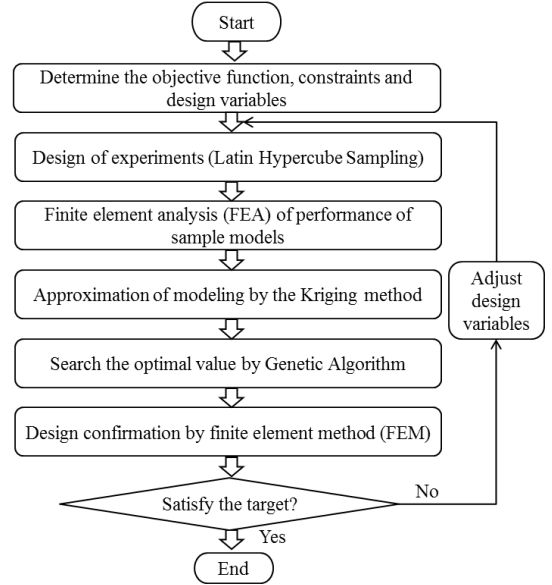


Fig. 7. Optimal design process.

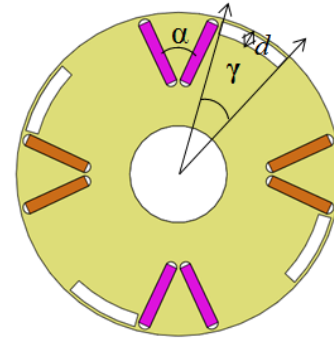


Fig. 8. Optimal design variables.

### III. OPTIMAL DESIGN

#### A. Optimal Design Process

Based on the proposed motor design strategy, an optimal design was performed to further improve torque and efficiency as shown in Fig. 7. Firstly, the objective functions, constraints and design variables were determined. Then the Latin Hypercube Sampling was applied in a Design of Experiment process for the selection of sampling points and the Kriging method performed for the approximation modeling. Using GA, optimal points for the design variables were obtained. Finally, the optimal design results were verified by FEM.

#### B. Objective Function, Constraints, and Design Variables

The objective functions for maximizing the torque and efficiency is shown in (5). The constraints are the magnet volume and UF of torque components as shown in (6). The design variables are shown in Fig. 8 and (7).  $\alpha$  is the V angle of magnet poles,  $\gamma$  is the span angle of the assisted barrier and  $d$  is the thickness of the assisted barrier.

- **Objective functions:**  
Maximize the average torque and efficiency (5)
- **Constraints:**  
Magnet volume = 75 cm<sup>3</sup>  
UF of reluctance torque ≥ 97%  
UF of magnetic torque ≥ 97% (6)

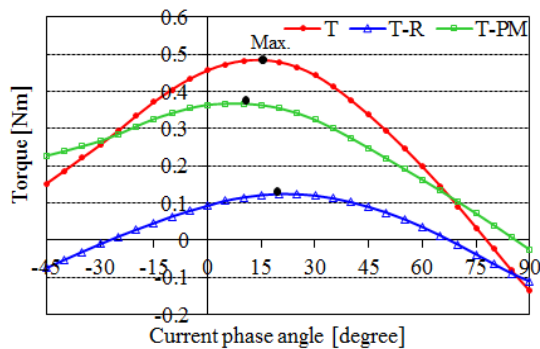


Fig. 9. Torque characteristics of the optimized motor. T: Resultant torque, T-PM: Magnetic torque, T-R: Reluctance torque.

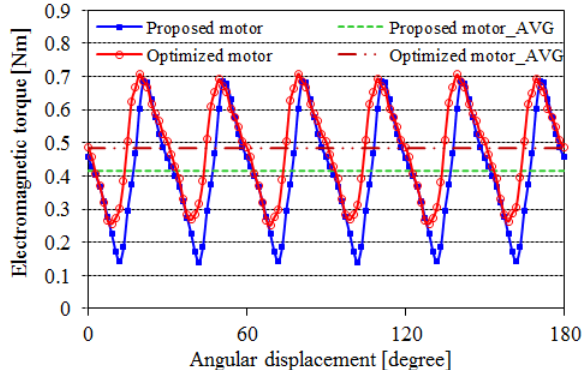


Fig. 10. Comparison of electromagnetic torque.

TABLE III  
COMPARISON OF PERFORMANCE DATA IN OPTIMAL DESIGN

Item	Unit	Proposed motor	Optimized motor
Max. torque (AVG)	Nm	0.416	0.485
UF of reluctance torque	%	100	97.8
UF of magnetic torque	%	100	98.8
Torque ripple	%	131.2	106.7
Output power	W	209.1	243.8
Copper loss	W	9.6	
Iron loss	W	15.28	14.20
Efficiency	%	89.4	91.1

- *Design variables:*  
 $45^\circ \leq \alpha$  (*V angle of magnets*)  $\leq 120^\circ$   
 $25^\circ \leq \gamma$  (*Span angle of assisted barrier*)  $\leq 40^\circ$  (7)  
 $1 \text{ mm} \leq d$  (*Thickness of assisted barrier*)  $\leq 4 \text{ mm}$

C. Optimal Design Results

The optimal design variables for the optimized motor are  $\alpha = 83^\circ$ ,  $\gamma = 26^\circ$ , and  $d = 3.4 \text{ mm}$ , respectively. Fig. 9 shows the torque characteristics of the optimized motor. The reluctance torque and the magnetic torque reach a maximum near the same current phase angle. The comparison of electromagnetic torque (Max.) between the proposed motor and the optimized motor is shown in Fig. 10. Compared with the proposed motor, the maximum torque of the optimized motor is increased by 16.6% and the efficiency is increased by 1.9%, while the torque ripple is decreased by 18.7%. The comparison of detailed performance data between the proposed motor and the optimized motor are listed in Table III.

IV. CONCLUSION

This paper has proposed a new rotor optimal design strategy for V-type IPM motors. The proposed motor adopts assisted barriers between two adjacent magnet poles aiming at improving the torque characteristics by making the reluctance torque and the magnetic torque reach a maximum near or at the same current phase angle. Firstly, a concept design using iterative optimization has been performed for demonstrating the design principle as well as verifying the advantage of the technique. Then the optimal design using Kriging method and GA was applied for further improvement. As the results show, the final optimized motor with assisted barriers demonstrates good performance with improved torque and efficiency as well as reduced torque ripple. It can be concluded that the proposed technique is an effective and competitive approach to the design of high performance PM motors where magnetic saliency exists.

ACKNOWLEDGMENT

This research was supported by BK21PLUS program through the National Research Foundation of Korea funded by the Ministry of Education.

REFERENCES

- [1] F. Parasiliti, M. Villani, S. Lucidi, and F. Rinaldi, "Finite element based multi-objective design optimization procedure of interior permanent magnet synchronous motors for wide constant-power region operation," *IEEE Trans. Ind. Electron.*, vol. 59, no. 6, pp. 2503–2514, Jun. 2012.
- [2] S. Kim, Y. Kim, G. Lee and L. Hong, "A novel rotor configuration and experimental verification of interior pm synchronous motor for high speed applications," *IEEE Trans. Magn.*, vol. 48, no. 2, pp. 843-846, 2012.
- [3] C. S. Jin, D. S. Jung, K. C. Kim, Y. D. Chun, H. W. Lee, and J. Lee, "A study on improvement magnetic torque characteristics of IPMSM for direct drive washing machine," *IEEE Trans. Magn.*, vol. 45, no. 6, pp. 2811–2814, Jun. 2009.
- [4] P. Zhang, D. M. Ionel, and N. A. O. Demerdash, "Morphing parametric modeling and design optimization of spoke and V-type permanent magnet machines by combined design of experiments and differential evolution algorithms," *IEEE IAS Energy Conversion Congress and Exposition (ECCE)*, pp. 5056-5063, Sep. 2013.
- [5] K. Yamazaki, M. Kumagai, T. Ikemi, and S. Ohki, "A Novel Rotor Design of Interior Permanent-Magnet Synchronous Motors to Cope with Both Maximum Torque and Iron-Loss Reduction," *IEEE Trans. on Ind. Appl.*, vol. 49, no. 6, pp. 2478-2486, Nov. / Dec. 2013.
- [6] R. Akaki, Y. Takahashi, K. Fyjiwara, and M. Matsushita, "Effect of Magnetic Property in Bridge Area of IPM Motors on Torque Characteristics," *IEEE Trans. Magn.*, vol. 49, no. 5, pp. 2335-2338, May 2013.
- [7] H. S. Chen, D. G. Dorrell, and M. C. Tsai, "Design and operation of interior permanent-magnet motors with two axial segments and high rotor saliency," *IEEE Trans. Magn.*, vol. 46, no. 9, pp. 3664–3675, Sep. 2010.
- [8] P. Alotto, M. Barcaro, N. Bianchi, and M. Guarnieri, "Optimization of interior pm motors with machaon rotor flux barriers," *IEEE Trans. Magn.*, vol. 47, no. 5, pp. 958–961, May 2011.
- [9] M. Popescu, D. M. Ionel, T. J. E. Miller, S. J. Dellinger, and M. I. McGilp, "Improved finite element computations of torque in brushless permanent magnet motors," *Inst. Electr. Eng. Proc.—Electr. Power Appl.*, vol. 152, no. 2, pp. 271–276, 2005.
- [10] W. Q. Chu, and Z. Q. Zhu, "Average torque separation in permanent magnet synchronous machines using frozen permeability," *IEEE Trans. Magn.*, vol. 49, no.3, pp. 1202-1210, Mar. 2013.